Organic Tissues in Rotating Bioreactors: Fluid-Mechanical Aspects, Dynamic Growth Models, and Morphological Evolution

Marcello Lappa

Microgravity Advanced Research and Support Center, Via Gianturco 31-80146, Napoli, Italy; telephone: +39-81-6042591; fax: +39-81-6042100; e-mail: lappa@marscenter.it

Received 9 December 2002; accepted 23 July 2003

Published online 24 September 2003 in Wiley InterScience (www.interscience.wiley.com). DOI: 10.1002/bit.10821

Abstract: This analysis deals with advances in tissue-engineering models and computational methods as well as with novel results on the relative importance of ''controlling forces'' in the growth of organic constructs. Specifically, attention is focused on the rotary culture system, because this technique has proven to be the most practical solution for providing a suitable culture environment supporting three-dimensional tissue assemblies. From a numerical point of view, the growing biological specimen gives rise to a moving boundary problem. A ''volume-of-fraction'' method is specifically and carefully developed according to the complex properties and mechanisms of organic tissue growth and, in particular, taking into account the sensitivity of the construct/liquid interface to the effect of the fluid-dynamic shear stress (it induces changes in tissue metabolism and function that elicit a physiological response from the biological cells). The present study uses available data to introduce a set of growth models. The surface conditions are coupled to the transfer of mass and momentum at the specimen/culture-medium interface and lead to the introduction of a group of differential equations for the nutrient concentration around the sample and for the evolution of tissue mass displacement. The models are then used to show how the proposed surface kinetic laws can predict (through sophisticated numerical simulations) many of the known characteristics of biological tissues grown using rotating-wall perfused vessel bioreactors. This procedure provides a validation of the models and associated numerical method and also gives insight into the mechanisms of the phenomena. The interplay between the increasing size of the tissue and the structure of the convective field is investigated. It is shown that this interaction is essential in determining the time evolution of the tissue shape. The size of the growing specimen plays a critical role with regard to the intensity of convection and the related shear stresses. Convective effects, in turn, are found to impact growth rates, tissue size, and morphology, as well as the mechanisms driving growth. The method exhibits novel capabilities to predict and elucidate experimental observations and to identify cause-and-effect relationships. © 2003 Wiley Periodicals, Inc. *Biotechnol Bioeng* **84:** 518–532, 2003.

Correspondence to: M. Lappa

Keywords: tissue engineering; rotating vessel; growth kinetics; fluid motion; mathematical models; moving boundary method; morphology evolution

INTRODUCTION

Given the current knowledge in growing organic tissues as model systems for controlled studies of tissue development, and the certain future developments in growing biological tissues as a potential source of functional constructs for organ repair, the concept of tissue engineering is nearing reality.

Tissue engineering is a new field that enables tissue equivalents to be created from isolated cells in combination with biomaterials and bioreactor culture vessels. Potentially it can provide a basis for systematic, controlled in vitro studies of tissue growth and function as well as detailed knowledge of many important problems, including the chemistry and mechanics of healthy organs and of cancers, infectious diseases, immune system failures, etc. Moreover, the constructs obtained by these techniques will someday be used for treatment of damaged human tissues and/or healthy organs.

A key factor in this new field of engineering involves how to define the properties of the artificial environments wherein biological tissues are grown in order to achieve the best possible conditions for growth. Organic tissues are very sensitive to their environment and, if exposed to sufficiently severe conditions, may denature and/or degrade. Often, they must be constantly maintained in a thoroughly hydrated state at or near physiological pH and temperature. For these reasons, very gentle and restricted techniques have been used by investigators.

A challenge that has plagued tissue science throughout its short history, however, is that most of these gentle cell-culture techniques produce flat, one-cell-thick specimens that offer limited insight into how cells work together. Moreover, without a proper three-dimensional (3D) assembly, epithelial cells (the basic cells that differentiate tissue into specific organ functions) lack the proper clues for growing into the variety of cells that make up a particular tissue.

The most promising method to solve these problems seems to be the rotating-wall perfused vessel bioreactor (RWPV), a can-like vessel equipped with a membrane for gas exchange and ports for media exchange and sampling. As the bioreactor turns, the cells continually fall through the medium. Under these quiet conditions, the cells ''self-assemble'' to form clusters that sometimes grow and differentiate much as they would in the body. Thus, the fluid medium neutralizes most of gravity's effects and encourages cells to grow naturally. In fact, the rotating bioreactor was invented as a model of microgravity effects on cells.

Ground tests of the bioreactor have yielded 3D biological specimens approximating natural growth, a striking change from the pancake shapes of traditional cultures. As cells replicate, they ''self-associate'' to form a complex matrix of collagens, proteins, fibers, and other chemicals. Eventually, on Earth, the clusters become too large to fall slowly, which demonstrates that research must be continued in the true weightlessness of space.

Excellent and surprising experiments were carried out by Freed et al. (1997), who grew specimens of bovine cartilage tissue under both normal (Earth) and microgravity conditions (Mir), and reported that initially disk-like specimens became spherical in space, whereas constructs grown on Earth maintained their initial disk shape. Experience aboard Mir turned microgravity bioreactor research into a mature science and proved that the gravity effect may play a crucial role in determining the properties and the growth conditions of organic tissues.

Further progress in creating proper environments for the growth of the tissues requires an understanding of how chemical, mechanical, and other environment factors influence growth. Recent advances in cellular and molecular biology have furthered our knowledge of the biochemical aspects of this problem. Moreover, theories have been proposed to take into account mechanical factors.

According to some investigators (Rodriguez et al., 1994; Taber, 1998a, 1998b; Taber and Chabert, 2002), growth and remodeling in tissues may be modulated by mechanical factors such as internal stress. A general continuum formulation for finite volumetric growth in soft elastic tissues, based on their internal ''mechanical state,'' has thus been proposed. This dependence has been introduced through the so-called ''growth law,'' which is a constitutive equation for the rate of change of the growth tensor, and describes its dependence on mechanical quantities such as stress, strain, and strain energy. The growth tensor is determined from the growth law. Two excellent implementations of this theory have been used to model continuous growth of soft tissues. The first, developed by Taber and coworkers (Taber, 1998a, 1998b; Taber and Chabert, 2002), has been used to investigate the growth of the heart, arteries, and skeletal muscles. In this approach, the growth law was defined on an initial fixed reference configuration for the entire growth process. In the second method, proposed by Rodriguez et al. (1994), the growth model was defined on the current configuration of the loaded, growing material. This method was used to elucidate how residual stress arises during growth and how, in turn, growth is affected by stress in the tissue.

Other theories have focused on the transport of gas in the culture medium surrounding the growing tissue, because it is proposed that this factor also may be important. The role played by the supply of gas on the rates of synthesis was modeled by Obradovic et al. (2000). They developed an excellent model taking into account the transport of dissolved oxygen in the feeding solution and, in particular, the effect of the gas tension. It was found that more efficient gas transport in both the culture medium and at the construct surfaces stimulates rapid tissue growth, whereas cultivation at low oxygen tension has the reverse effect.

The basic approach used in these theories was to combine published experimental results with relatively simple theoretical models. First, trends in the data available are used to postulate qualitatively biomechanical principles for growth. Then, explicit growth laws are proposed and tested for their ability to predict known patterns of growth, leading to important theoretical results and agreement with the experiments.

It is important to stress that the available ''mechanical'' theories have focused on what happens inside the tissue, whereas the biomechanical laws that govern soft tissue growth in terms of surface incorporation/conversion conditions (interface kinetics of the growth) remain poorly understood. Superimposed on this is the poor state of our current understanding of the effect of ''fluid-dynamic'' shear forces. In contrast, on the basis of experimental results (Freed et al., 1997), these effects seem to play a crucial role in determining the final shape and the size of the specimens.

The aims of the present study are: (1) to introduce a mathematical model to handle the complex phenomena related to the growth of organic tissues that takes into account (a) the main features of the bioreactor used for growth (in particular, the fluid-dynamics), (b) the transport of nutrients in the feeding solution and how they are converted in biological tissue, and (c) the mass variation of the specimen; (2) to shed some light on the complex interplay between the increasing size of the tissue and the structure of the convective field inside the reactor; (3) to make available to the scientific community a numerical method based on this model; (4) to validate the model through comparison of the numerical results with well-known and important experimental ones.

The present investigation is the first attempt to analyze in detail these (fluid-dynamic) behaviors.

MATERIALS AND METHODS

The Rotating Vessel

This rotating vessel device was developed by NASA within the framework of the ideas and concepts originally pointed

out in the pioneering works of Briegleb (see, e.g., Briegleb [1988], fast-rotating clinostat technique). Already, by the early 1960s, Briegleb recognized the need to study the influence of weightlessness on living cells. Access to real weightlessness was always very limited, but Briegleb and coworkers (Briegleb, 1988, 1992; Hemmersbach-Krause et al., 1993) became the first to use a fast-rotating clinostat for research with single mammalian cells and unicellular organisms under functional weightlessness. In their studies, two fast-rotating clinostat microscopes (CLIMIs) were constructed, which were subsequently used by other investigators (Cogoli, 1992; Kordyum, 1994; Todd and Gruener, 1992).

Cells derived from diverse tissue sources lose their specialized features and dedifferentiate when grown under traditional two-dimensional cell culture conditions. Over the years suspension culture has become the most popular method of preventing this problem. There is now a rich and diverse selection of available culture vessels for suspension culture (Hammond and Hammond, 2001).

Several recent reviews have summarized the use of suspension culture (Helmrich and Barnes, 1998), scale-up of suspension culture for industrial use (Mather, 1998), application to anchorage-dependent cells by the use of microcarriers (Gao et al., 1997a; Pollack et al., 2000), and automation of roller-bottle forms of suspension culture (Kunitake et al., 1997).

NASA investigators brought together the various elements of suspension culture (continuous sedimentation of particles through culture medium, suspension of cells and microcarriers without inducing turbulence, a rotating-wall vessel, and a coaxial oxygenator to allow gas exchange by dissolved gases without undesired bubbles) for the first time. This led to an efficient (but simple) design for suspension culture vessels embodied in the rotating-wall perfused vessel, a horizontally rotating cylindrical culture vessel with a coaxial tubular oxygenator (Fig. 1). These vessels have characteristic features that determine their utility. First, fluid flow is near solid body at most operating conditions. If the inner and outer cylinders of the rotating-wall vessel rotate at the same angular velocity (rpm), then the (radial) laminar-flow fluid velocity gradient would be minimized. Second, the culture medium is gently mixed by rotation, avoiding the necessity for stirring vanes. The mixing is the result of a secondary flow pattern induced by particle sedimentation through the fluid media (at gravity conditions) or by laminar flows established when differential rotation rates are chosen for the vessel components (microgravity conditions).

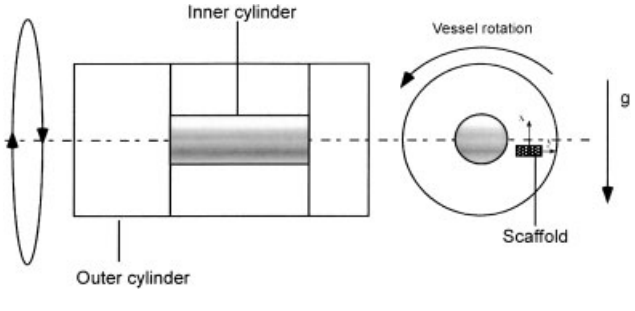

Figure 1. Sketch of the rotating bioreactor (on-ground conditions).

The rotating-wall perfused vessel was invented to grow cells in space, with the additional benefit of working in Earth's gravity. It simulates the weightless environment of space while on Earth by putting biological constructs in a growth medium that constantly rotates and keeps them in endless freefall.

Clearly, the rotating vessel does not actually cancel gravity, but ideally maintains continual freefall conditions similar to those experienced by astronauts in the microgravity of space. Earth-based bioreactor cultures typically maintain cell growth for at least 60 days. On Earth, a sample then becomes so large (about 1 cm) that it is no longer suspended. In long-duration space missions, large-sample growth in bioreactors can be investigated to assess extended growth.

Due to the different technique used to guarantee mixing of nutrients in the feeding solution (dynamic seeding of constructs through the liquid posed in solid body rotation on Earth and differential rotation of the inner and outer vessel walls in space) the structure of the flow field changes completely according to the environment (normal gravity or microgravity conditions).

Within the framework of the aforementioned argument, this study aims to shed light on the surprising experimental results obtained by Freed et al. (1997). In particular, attention is focused on on-ground conditions, because most of the available experimental data for tissue engineering come from on-ground experimentation.

To optimize suspension culture, these aspects need to be expressed in simple mathematical relationships, and then quantitated and controlled.

Experiments and Terminal Velocity

The RWPV approach involves seeding cells onto 3D polymer scaffolds. The cell/scaffold constructs are placed in the rotating bioreactor that supplies the cells with nutrients and gases and removes wastes. The scaffold induces cell differentiation and degrades at a defined rate (it slowly biodegrades as the cells develop into a full tissue), whereas the bioreactor maintains controlled, in vitro culture conditions that permit tissue growth and development.

Concentration gradients within the bioreactor are minimized by the convection associated with gravitational construct settling during solid body rotation of the bioreactor in unit gravity. The vessel is rotated as a solid body in a horizontal plane around its central axis. The rotation rate can be adjusted so as to suspend each tissue construct about a fixed position within the vessel as viewed by an external observer (Obradovic et al., 2000). This condition guarantees dynamic equilibrium of the operative forces gravity, buoyancy, and drag, while maintaining each tissue construct in a

state of continuous freefall. Thus, a tissue construct falling through the culture media in the RWPV is fed as it effectively sieves through the nutrient media.

On Earth, the settling of diskoid scaffolds tends to align their flat, circular areas perpendicular to the direction of motion (Freed et al., 1997). To minimize shear and turbulence, usually the terminal velocity of the constructs is minimized by choosing scaffolds and culture media as close in density as possible.

Many data on the fluid-dynamic environment in rotating-wall perfused vessel bioreactors can be found in the excellent analyses done by Kleis et al. (1990), Wolf and Schwartz (1991, 1992), Gao et al. (1997a, 1997b), Meaney et al. (1998), Begley and Kleis (2000), Pollack et al. (2000), Hammond and Hammond (2001), and Coimbra and Kobayashi (2002).

These studies concern mainly the case of ''small'' aggregates, however, which have motion and dynamics that are quite different from those of the ''large'' constructs cultivated by Freed et al. (1997). Many investigators make cell aggregates rotate around the core of the vessel instead of allowing them to hover at fixed points. For the sake of completeness it should be pointed out that particles cultivated in suspension culture generally do not maintain an approximately steady position within the vessel, but rather they follow almost circular trajectories. Also, under these conditions, some equilibrium positions would exist within the reactor (these special points behave as ''attractors'' for the particles). In this case, however, tangential Coriolis-induced motion is significant and leads to spiraling of particles in the fluid stream with respect to a laboratory reference frame. Due to this effect, small particles tend to fall on large-radius orbits, which periodically strike the vessel wall.

In the case of relatively large cell aggregates and/or large scaffolds the behavior may be different, as demonstrated by Freed et al. (1997). Under some conditions the rotation rate can be adjusted so as to let each tissue construct ''hover'' about a stationary position with respect to a laboratory reference system (present case), even if small oscillations with respect to this position and impact with the wall may occasionally occur. For this case, many (quasi-stable) equilibrium positions are possible between the central oxygenator and the lowest portion of the wall (see Fig. 1). The prefix ''quasi'' is used because the constructs actually ''circulate'' in small loops around the aforementioned stationary fixed positions, due to the characteristic hydrodynamic patterns of disk settling. Gao et al. (1997a) noted that suspension of the scaffolds has a ''periodic nature''; however, because the oscillations of the relative velocity are slight (in agreement with the present assumptions), they concluded that this value may be assumed almost constant.

For these reasons, we simulate the experiments of Freed et al. (1997) and Obradovic et al. (2000); a simplified model is assumed, based on the results of Clift et al. (1978). In the range $1 < \mathrm{Re} < 10^3$, the terminal velocity, U, of a cylinder having diameter d and thickness L (aspect ratio $E = L/d$), free-falling with its symmetry axis parallel to the direction of motion (and of gravity) through a liquid with kinematic viscosity, ν, can be computed according to:

$$C_D \mathrm{Re}^2 = \frac{2g\Delta\rho E d^3}{\rho\nu^2} \tag{1a}$$

$$C_D = \frac{64}{\pi \mathrm{Re}}(1 + 0.138\,\mathrm{Re}^{0.792}) \tag{1b}$$

where $\Delta\ \rho$ is the density gradient between the cylindrical body and the surrounding fluid and:

$$\mathrm{Re} = \frac{Ud}{\nu}$$

is the diameter-based Reynolds number (Re) associated with dynamic construct sedimentation. These equations provide a simple and efficient method for computation of terminal velocity. Clearly, the direction of motion is not exactly parallel to the direction of gravity as assumed by Eqs. (1a) and (1b). Generally, the terminal velocity vector has a component along the direction of gravity and also a perpendicular component. The latter is small, however, and for this reason it is not taken into account in the present computations, even if it could explain some weak deviations with respect to the axisymmetric shape that sometimes characterize the specimen (see Numerical Simulations subsection).

Under these assumptions, the mechanism of equilibrium is very simple: The net weight of the tissue is balanced by the viscous resistance and the flow around the construct is axisymmetric [Eq. (1a) and (1b)]. According to Galileo's invariance principle, this situation corresponds (see Numerical Simulations) to the specimen at rest as seen in a laboratory frame and the fluid moving upward in the direction opposite to the gravity force with velocity equal to U.

Other effects such as Coriolis forces can be considered negligible for the dynamics of the scaffold/construct because the major direct determinants of the terminal velocity in this case are gravity and viscous resistance (see Hammond and Hammond, 2001).

In the experiments done by Freed et al. (1997) and Obradovic et al. (2000) cartilage was used as a model musculoskeletal tissue. Cartilage was selected because of its resilience and low metabolic requirements. Their method was based on cartilage cells (chondrocytes) and biodegradable polyglycolic acid (PGA) scaffolds of cylindrical shape. Chondrocytes were isolated from bovine calf articular cartilage and seeded onto the fibrous, biodegradable polyglycolic acid scaffolds (these disk-like structures mimic the body's internal environment). PGA scaffolds (the same material used to make Dexon absorbable surgical sutures) were 0.5-cm-diameter × 0.2-cm-thick disks formed as a 97% porous mesh of 13-μm-diameter fibers. Culture medium consisted of Dulbecco's modified Eagle medium (DMEM) with 4.5 g/L glucose and other substances (see Freed et al. [1997] for further details on the composition of the culture medium).

For this case, the density difference between the construct and the feeding solution was:

$$\Delta\rho = 4.9\,10^{-2}[\mathrm{g\,cm^{-3}}] \rightarrow \frac{2g\Delta\rho E d^3}{\rho\nu^2} = 7.4\,10^4$$

Eqs. (1a) and (1b), solved using a Newton–Raphson method, give:

$$\mathrm{Re} = \frac{Ud}{\nu} = 290 \rightarrow U = 4.64\,[\mathrm{cm/s}]$$

and this velocity is in agreement with the average vessel rotation rate ($\cong$ 30 rpm; see Obradovic et al. [2000]) that was used by the investigators to maintain each tissue construct floating at an approximately steady position within the vessel. In fact, the bioreactor was configured as the annular space between a 5.75-cm-diameter polycarbonate outer cylinder and a 2-cm-diameter hollow inner cylinder with a porous wall. This corresponds to an average fluid velocity of $\cong$ 6 cm/s, which is in reasonable agreement with the terminal velocity computed according to Eqs. (1a) and (1b).

Mathematical Models and Numerical Technique

From a numerical point of view, the growing tissue gives rise to a moving boundary problem. Moving boundary problems remain a challenging task for numerical simulation, prompting much research and leading to many different solutions.

The numerical simulations of these problems require a discretization or nodalization to allow numerical treatment on computers. There are two fundamentally different approaches. On the one hand, Eulerian methods use a frame of reference (discretization grid or mesh, control volumes, etc.) fixed in space, and matter moving through this frame of reference. Lagrangian methods, on the other hand, use a frame of reference (marker particles) fixed to and moving with the matter.

The first method capable of modeling multiphase flow, separated by a moving interface, was the marker and cell (MAC) of Harlow and Welch (1965). This is in fact a combination of a Eulerian solution of the basic flow field, with Lagrangian marker particles attached to one phase to distinguish it from the other phase. Although the staggered mesh layout and other features of the MAC have become a model for many other Eulerian codes, the marker particles proved to be computationally too expensive and have been rarely used.

In the specific case of growth of organic tissues from feeding solutions, and in order to introduce novel numerical techniques, one must generally accomplish at least two things simultaneously: (a) determine the concentration field of nutrients in the liquid phase; and (b) determine the position of the interface between the tissue and the culture medium. According to the technique used to address (a) and (b), in principle, the numerical procedures able to solve these problems can be divided into two groups:

1. Multiple region solutions utilizing independent equations for each phase and coupling them with appropriate boundary conditions at the tissue/liquid interface. This approach to the problem takes the point of view that the interface separating the bulk phases is a mathematical boundary of zero thickness where interfacial conditions are applied. These interfacial conditions couple to the concentration equations in the bulk and this system of equations and boundary conditions provides a means to address (a) and (b). Difficulties arise when this technique is employed, because, in this case, in the vicinity of the growing construct front (phase change), conditions of mass flux and velocity evolution must be accounted for. This effectively rules out application of a fixed-grid numerical solution, because deforming grids or transformed coordinate systems are required to account for the position of the tissue surface.
2. Single region (continuum) formulations (or ''phase-field'' models), which eliminate the need for separate equations in each phase, by establishing conservation equations that are universally valid. Theoretically, the major advantage of single region formulations is that they do not require the use of quasi-steady approximations, numerical remeshing, and coordinate mapping.

In a phase-field model, a phase-field variable, ϕ, which varies in space and time is introduced to characterize the phase of the material. In place of the ''sharp'' transition from biological constructs to feeding liquid that would characterize the multiple region formulations, here the phase-field varies smoothly but rapidly through an interfacial region. In addition, in place of the interfacial jump conditions used in the multiple description, a differential equation applied over the entire computational domain governs the evolution of ϕ. The effect is a formulation of the free boundary problem that does not require the explicit application of interfacial conditions at the unknown location of a phase boundary, which is why this strategy has been adopted in the present study.

The first method capable of modeling complex multiphase flow separated by a moving interface, and capable of undertaking a fixed-grid solution without resorting to mathematical manipulations and transformations, was the aforementioned marker and cell (MAC) of Harlow and Welch (1965). Instead of MAC, however, volume-of-fluid methods (VOF) and level-set methods have became popular in recent years. (For a very comprehensive discussion dealing with the genesis and evolution of these Eulerian methods, see Rider and Kothe [1998], Sethian [1999], Osher and Fedkiw [2002], and Gueyffier et al. [1999].) In particular, these approaches have had widespread use for the simulation of typical problems associated with gas/liquid or liquid/liquid systems where surface tension effects play a ''critical role'' in determining the shape of the fluid/fluid interface and/or its motion. On the other hand, ''enthalpy methods'' and similar techniques, taking into account the release or absorption of latent heat, have been successfully applied to the case of thermal phase change problems characterized by the presence of moving solid/melt interfaces, due to the heating or the cooling of the system under

investigation (Beckermann et al., 1999; Bennon and Incropera, 1987; Kim et al., 2000; Kothe et al., 1997; Lappa and Savino, 2002; Udaykumar et al., 1999).

Nevertheless, a complete numerical method aimed at the (''moving boundary'') simulation of growth of biological constructs in the frame of the new field of tissue engineering is still missing.

Organic Tissue Growth Volume-of-Fraction Method (OTGVOF)

The OTGVOF method, which, similar to VOF and enthalpy methods, is a single region formulation, allows a fixed-grid solution to be undertaken, and is therefore able to utilize standard solution procedures for the fluid-flow and species equations directly, without resorting to mathematical manipulations and transformations.

This method accounts for the organic solid mass stored in the generic computational cell by assigning an appropriate value of ϕ to each mesh point ($\phi = 1$ biological tissue, $\phi = 0$ feeding solution, and $0 < \phi < 1$ for an interfacial cell). The key element for the OTGVOF method is its technique for adjourning ϕ. Upon changing phase, the ϕ-value of the cell is adjusted to account for mass absorption, with this adjustment being reflected in the concentration distribution of nutrients in liquid phase as a sink. The modeling of these phenomena leads to the introduction of a group of differential equations, strictly related, from a mathematical point of view, to the ''kinetic conditions'' used to model mass transfer at the tissue surface.

Several studies have shown that growth rates are sensitive to many parameters, including temperature, defect formation, shear forces, surface orientation, etc. This problem is very complex and poorly understood.

Growth proceeds by the incorporation of growth units (atoms, molecules, or small aggregates) from the feeding solution to the biological construct. Nutrients available in the culture medium are incorporated and converted into the tissue main components. This incorporation produces a concentration depletion zone around the specimen. The size and shape of the depletion zone are controlled by the coupled transport of the feeding species in solution to the growing surface and the processes allowing these species to be ''incorporated'' into the tissue matrix.

In the case of protein crystals (Lappa, 2003; Pusey et al., 1986; Rosenberger, 1986), it is well known that the growth rate (i.e., the surface growth kinetics) depends on the steepness of the feeding concentration gradient and that this gradient, in turn, depends on the degree of supersaturation. By analogy with these models it is reasonable to assume that the concentration of nutrient at the tissue surface must satisfy a condition, such as:

$$D\left.\frac{\partial C}{\partial n}\right|_i = \lambda C_i \tag{2}$$

where C_i is the concentration of the nutrient (in the experiments of Freed et al. [1997] it is glucose) at the construct/liquid interface, D is the related diffusion coefficient, λ is a ''kinetic coefficient'' having the dimensions of a velocity (e.g., centimeters per second), and n denotes the direction perpendicular to the sample surface. In the case of biological tissue growth, the role played in the case of organic crystals by the degree of supersaturation has to be replaced by the local value of concentration of nutrient in liquid phase.

The growth rate (e.g., Lappa, 2003; Pusey et al., 1986) is defined as:

$$\theta = \left.\frac{D}{\rho_s}\frac{\partial C}{\partial n}\right|_i \tag{3}$$

where ρ_s is the total density of the solution and C satisfies Eq. (2).

If $C_i = 0$, no net increase in the proportion of solid phase can accrue because nutrients are not available (the tissue does not grow). In contrast, if $C_i > 0$, tissue growth occurs and the rapidity of the phenomena is driven by the value of the kinetic coefficient, λ.

Note that this model, introduced herein by analogy with models for organic crystal growth, ignores the fact that, according to biomechanical growth laws proposed in the case of soft tissues (Fung, 1990; Taber, 1998), the rate of growth must depend on the stresses. For instance, the fluid shear stresses generated by blood flow in the vasculature can profoundly influence the phenotype of the endothelium by regulating the activity of certain flow-sensitive proteins (e.g., enzymes) as well as by modulating gene expression (Topper and Gimbrone, 1999). This ''physical force'' can induce changes in cell metabolism and function. In particular, for the case under investigation, the stress environment can elicit a physiological response from the cells, representing the building blocks of the construct and causing production of extracellular matrix (ECM).

To model these aspects, the kinetic condition is rewritten as:

$$D\left.\frac{\partial C}{\partial n}\right|_i = \lambda(a\tau)^{1/2} C_i \tag{4}$$

where a is a constant (having the reciprocal units of the shear stress) and τ is the fluid-dynamic shear stress at the tissue/liquid interface.

Therefore, the growth rate is:

$$\theta = \lambda(a\tau)^{1/2} C_i/\rho_s$$

with C satisfying Eq. (4). This condition finally takes into account the main aspects of growth behavior; that is, the availability of nutrients (C_i), the slow surface kinetics (λ), and the intriguing effect of surface shear stress (τ).

Selection of the exponent (hereafter referred to as e) for the shear stress in Eq. (4) was based on a parametric investigation: Several simulations of the experiments by Obradovic et al. (2000) have been carried out for different values of the exponent, $e = n$ and $e = 1/n$ ($n = 1,2,3,4$, etc.). This method has shown that $e = 1/n$, $n = 2$ (other values do not reproduce the experiments). The parametric investiga-

tion is not shown in detail for the sake of brevity. It is worthwhile to emphasize how, according to Eq. (4), the growth phenomena depend on both transfer of mass and momentum to the tissue surface.

Governing Field Equations

In the presence of convection, the flow is governed by the continuity, Navier–Stokes, and species equations, which, in nondimensional, conservative form, read:

$$\underline{\nabla} \cdot \underline{V} = 0 \tag{5}$$

$$\frac{\partial \underline{V}}{\partial t} = -\underline{\nabla} p - \underline{\nabla} \cdot [\underline{V}\,\underline{V}] + S_c \nabla^2 \underline{V} - S_c \frac{1}{\eta} \underline{V} \tag{6}$$

$$\frac{\partial C}{\partial t} = [-\underline{\nabla} \cdot (\underline{V} C) + \nabla^2 C] \tag{7}$$

where $S_c = \upsilon/D$ is the Schmidt number (υ is the kinematic viscosity of the culture liquid). The nondimensional form of the equations results from scaling the lengths by a reference distance (L = 1 cm); the time by L^2/D; velocity, V, and pressure, p, by D/L and D^2/L^2, respectively; and the initial value of the nutrient is $C_{(o)}$. Note that concentrations are not posed in nondimensional form (grams per cubic centimeter).

Assumptions invoked in the development of equations for this continuum model include: laminar flow, Newtonian behavior of the phases (this implies that the constructs, should be treated as highly viscous fluids), and constant phase densities.

Moreover, the tissue is assumed to be nondeforming and free of internal stress, whereas the multiphase region (region where nutrients are absorbed and increase of mass occurs) is viewed as a porous material characterized by an isotropic permeability, η. The term $-S_c V/\eta$ in Eq. (6) is the Darcy term added to the momentum equation to damp convection in the solid phase. In the present analysis, permeability is assumed to vary according to the Carman–Kozeny equation (Bennon and Incropera, 1987; Lappa and Savino, 2002):

$$\eta = \frac{(1 - \phi + \varepsilon)^3}{(\phi + \varepsilon)^2}$$

with $\varepsilon = 10^{-5}$. In practice, the effect of η is as follows: in full liquid elements $1/\eta$ is very small and has no influence; in elements that are changing phase the value of $1/\eta$ will dominate over the transient, convective, and diffusive components of the momentum equation, thereby forcing them to imitate the Carman–Kozeny law; and in totally solid elements the final large value of $1/\eta$ will swamp out all terms in the governing equations and force any velocity predictions effectively to zero.

Because the momentum and species equations are valid throughout the entire domain, explicit consideration need not be given to boundaries between solid, multiphase, and liquid regions.

Phase-Field Equation

On the surface of the tissue:

$$(|\,\underline{\nabla}\,|\,\phi \neq 0,\ 0 < \phi < 1)$$

and nutrient concentration must satisfy the kinetic condition that, in nondimensional form, reads:

$$\left.\frac{\partial C}{\partial n}\right|_i = \tilde{\lambda}(\tilde{a}\tilde{\tau})^{1/2}(C_i) \tag{8}$$

where:

$$\tilde{\lambda} = \lambda L/D,\ \tilde{\tau} = \left(\frac{\partial u}{\partial y} + \frac{\partial v}{\partial x}\right)$$

with u and v being the velocity components along x and y, respectively.

In Eq. (8), the concentration gradient can be computed as:

$$\frac{\partial C}{\partial n} = \underline{\nabla} C \cdot \underline{\hat{n}} \tag{9}$$

where $\underline{\hat{n}}$ is the unit vector perpendicular to the construct/liquid interface pointing into the culture medium:

$$\underline{\hat{n}} = -\frac{\underline{\nabla}\phi}{|\underline{\nabla}\phi|} = (\alpha, \beta) \tag{10}$$

$$\begin{aligned} \alpha &= -\frac{\partial \phi}{\partial x} \Big/ \sqrt{\left(\frac{\partial \phi}{\partial x}\right)^2 + \left(\frac{\partial \phi}{\partial y}\right)^2}, \\ \beta &= -\frac{\partial \phi}{\partial y} \Big/ \sqrt{\left(\frac{\partial \phi}{\partial x}\right)^2 + \left(\frac{\partial \phi}{\partial y}\right)^2} \end{aligned} \tag{11}$$

because:

$$\frac{\partial C}{\partial n} = \alpha \frac{\partial C}{\partial x} + \beta \frac{\partial C}{\partial y}$$

(hereafter subscript i is omitted), and Eq. (8) can be written as:

$$\alpha \frac{\partial C}{\partial x} + \beta \frac{\partial C}{\partial y} = \tilde{\lambda}(\tilde{a}\tilde{\tau})^{1/2} C \tag{12}$$

where:

$$\tilde{\lambda}(\tilde{a}\tilde{\tau})^{1/2} C$$

represents the mass exchange flux between solid and liquid phase (i.e., tissue and feeding solution). The mass (tissue matrix coming from incorporation and conversion of nutrients) stored in computational cells that are undergoing phase change can be computed according to:

$$\frac{\partial M}{\partial t} = \frac{\lambda L^4}{D} (\tilde{a}\tilde{\tau})^{1/2} C\, ds \tag{13}$$

where ds is the ''reconstructed'' portion of the tissue surface (by definition, perpendicular to the interface normal vector, $\hat{n}$) ''bounded'' by the frontier of the control volume (computational cell) located astride the tissue surface.

To compute the nondimensional volume of the tissue mass stored in a grid cell, the details of the specific tissue under consideration must be introduced into the model.

Functional cartilaginous constructs for scientific research and eventual tissue repair were cultivated by Freed et al. (1997) in bioreactors starting from chondrocytes immobilized on polymeric scaffolds and fed by glucose. The scaffolds gradually degraded as the cells regenerated a cartilaginous tissue matrix consisting of water (soft tissues consist in fact primarily of various cell types, an extracellular matrix, and abundant water), glycosaminoglycan (GAG), and type II collagen (the main cartilage components).

Following Freed et al. (1997), the densities of these components in the tissue (partial densities) were found to be $\rho_{GAG} = 6 \cdot 10^{-2}$ g cm^{-3} and $\rho_{collagen} = 2.7 \cdot 10^{-2}$ g cm^{-3}, respectively.

The nondimensional volume of the tissue mass (GAG + collagen) stored in a grid cell can be computed as:

$$dv\Big|_{\text{stored}} = \frac{1}{L^3}\,\frac{M}{(\rho_{GAG} + \rho_{collagen})} \tag{14}$$

correspondingly:

$$\phi = \frac{dv|_{\text{stored}}}{dv} \tag{15}$$

where dv is the volume of the computational cell.

Therefore, the phase-field equation reads:

$$\frac{\partial \phi}{\partial t} = 0, \text{ if} |\underline{\nabla}\phi| = 0$$

$$\frac{\partial \phi}{\partial t} = \frac{\tilde{\lambda}(\tilde{a}\tilde{\tau})^{1/2}(C)ds}{(\rho_{GAG} + \rho_{collagen})\mathrm{d}r}, \text{ if } |\underline{\nabla}\phi| \neq 0,\ 0 < \phi < 1 \tag{16}$$

with C satisfying Eq. (12).

From mass balance, the solution for the normal velocity at the interface is:

$$\underline{V} \cdot \underline{\hat{n}} = (\rho_C/\rho_S)\theta^* \text{ if } |\underline{\nabla}\phi| \neq 0,\ 0 < \phi < 1 \tag{17a}$$

where ρ_S and ρ_C are the total density of the solution and the total density of the specimen, respectively, and the nondimensional growth rate (e.g., Pusey et al., 1986) is computed as:

$$\theta^* = \left(\frac{1}{\rho_S}\right)\frac{\partial C}{\partial n} = \tilde{\lambda}(\tilde{a}\tilde{\tau})^{1/2} C/\rho_S \tag{17b}$$

with C (glucose concentration) satisfying Eq. (12).

Eqs. (12), (16), and (17) act as ''moving boundary conditions,'' their solution being strictly associated with the computational check on the value of ϕ and its gradient. For instance, in the case of Eqs. (16), the phase variable, ϕ, is updated (i.e., $\delta\phi/\delta t \neq 0$) only where and $0 < \phi < 1$—that is, close to the tissue/solution interface where tissue enlargement occurs due to ''internal cell division'' and ''production of extracellular matrix.'' In contrast, ϕ does not change (i.e., $\delta\phi/\delta t = 0$) far from the surface. Note that, typically, for organic tissue growth, the normal velocity at the interface is very small with respect to the terminal velocity, and for this reason it can be neglected.

Discretization

Eqs. (5)–(7) subjected to the initial and boundary conditions are solved numerically in primitive variables by a control volume method. The domain is discretized with a uniform mesh and the flow-field variables defined over a staggered grid. Forward differences in time and upwind schemes in space (second-order accurate) are used to discretize the partial differential equations, resulting in (n superscript indicates time-step):

$$\underline{V}^{n+1} = \underline{V}^n + \Delta t[-\underline{\nabla}\cdot(\underline{V}\,\underline{V}) + Sc\nabla^2\underline{V}]^n - \Delta t\frac{S_c}{\eta}\underline{V}^{n+1} - \Delta t\underline{\nabla}p^n \tag{18}$$

$$C^{n+1} = C^n + \Delta t[-\underline{\nabla}\cdot[\underline{V}C] + \nabla^2 C]^n \tag{19}$$

The orientation of the surface of the crystal is used to determine the face fluxes for the computation of C at the crystal surface [Eq. (12)]. The interface orientation depends on the direction of the volume fraction gradient of the phase within the cell, and that of the neighbor cell (or cells) sharing the face in question.

The unit vector, $\underline{\hat{n}}$, results from the gradient of a smoothed phase field, $\phi\frown$, where the transition from one phase to the other takes place continuously over several cells (four or five). The smoothed phase field is obtained by convolution of the unsmoothed field, $\phi\frown$, with an interpolation function.

Depending on the interface's orientation, concentration gradients are discretized by forward or backward schemes. For this reason, Eq. (12) in discretized form reads (note that the i and j subscripts indicate the relative position along x and y, respectively, of the ''nodal'' values of C):

$$\alpha > 0,\ \beta > 0: \quad C_{i,j}^{n+1} = \frac{[\alpha\, C_{i+1,j}^{n+1}/\Delta x + \beta\, C_{i,j+1}^{n+1}/\Delta y]}{[\tilde{\lambda}(\tilde{a}\tilde{\tau})^{1/2} + \alpha/\Delta x + \beta/\Delta y]} \tag{20a}$$

$$\alpha < 0,\ \beta > 0: \quad C_{i,j}^{n+1} = \frac{[-\alpha\, C_{i-1,j}^{n+1}/\Delta x + \beta\, C_{i,j+1}^{n+1}/\Delta y]}{[\tilde{\lambda}(\tilde{a}\tilde{\tau})^{1/2} - \alpha/\Delta x + \beta/\Delta y]} \tag{20b}$$

$$\alpha > 0,\ \beta < 0: \quad C_{i,j}^{n+1} = \frac{[\alpha\, C_{i+1,j}^{n+1}/\Delta x - \beta\, C_{i,j-1}^{n+1}/\Delta y]}{[\tilde{\lambda}(\tilde{a}\tilde{\tau})^{1/2} + \alpha/\Delta x - \beta/\Delta y]} \tag{20c}$$

$$\alpha < 0,\ \beta < 0: \quad C_{i,j}^{n+1} = \frac{[-\alpha\, C_{i-1,j}^{n+1}/\Delta x - \beta\, C_{i,j-1}^{n+1}/\Delta y]}{[\tilde{\lambda}(\tilde{a}\tilde{\tau})^{1/2} - \alpha/\Delta x - \beta/\Delta y]} \tag{20d}$$

$$C_{i,j}^{n+1}$$

is computed from Eq. (20), then the phase variable is updated using Eq. (16):

$$\phi_{i,j}^{n+1} = \phi_{i,j}^{n} + \Delta t \frac{\tilde{\lambda}(\tilde{a}\tilde{\tau})^{1/2}(C_{i,j}^{n+1})\Delta s}{(\rho_{GAG} + \rho_{collagen})\Delta v} \qquad (21)$$

According to Eqs. (20) and (21), if the nutrient concentration is locally depleted and, correspondingly, the solid mass stored in the computational cell grows and the phase variable is increased. These phenomena are driven by the surface kinetic condition and by the shear-stress distribution; that is, the existing deposit grows if nutrient concentration is not zero and the mass exchange is proportional to the local value of the kinetic coefficient and of the fluid shear stress.

In Eq. (21), δs is the ''reconstructed'' portion of the solid wall. The determination of δs requires a well-defined ''interface-reconstruction'' technique. (The shape of the construct for a fixed time is not known a priori and must be determined as part of the solution; for instance, refer to the nonconnecting straight lines PLIC technique of Gueyffier et al. [1999].)

The solution procedure is summarized in the flow-scheme in what follows; it proceeds in four major stages:

1. Solution of the Navier–Stokes equations according to the MAC method [Eq. (18)]: $\underline{V}^{n+1}$ is computed as a function of $\underline{V}^{n}$.
2. Solution of the species equation [Eq. (19)]: C^{n+1} is computed as a function of the corresponding distribution and of $\underline{V}^{n}$.
3. Updating of the local values of C at the tissue/culture-medium interface according to Eqs. (20). This stage accounts for glucose depletion (due to incorporation into the tissue) at time $n + 1$.
4. Adjournment of the phase-field variable distribution. The phase-field variable is updated according to its distribution at the previous time-step (n) and on the basis of the newly computed values of concentration, C^{n+1}, at the construct interface [see Eq. (21)]. This final stage accounts for the increase in size of the specimen at time $n + 1$.

The implementation of the SMAC method for the solution of Eq. (18) is not described here for the sake of brevity (see Lappa and Savino, 1999). Parallel super-calculus is used due to the enormous time required for the computations (although the model is two-dimensional). The problem is split in two problems, one parabolic and the other elliptic. A parallel algorithm, explicit in time, is utilized to solve the parabolic equations (momentum and species equations). A parallel multisplitting kernel is introduced for the solution of the pseudo-pressure elliptic equation, representing the most time-consuming part of the algorithm. A grid-partition strategy is used in the parallel implementations of both the parabolic equations and the multisplitting elliptic kernel. A message-passing interface (MPI) is coded for interprocessor communications (for further details see, e.g., Lappa [1997] and Lappa and Savino [1999]).

Numerical Simulations

The equations and the initial and boundary conditions are solved numerically in cylindrical coordinates. The specimen (a disk-shaped cartilage construct having an initial size of 5 mm × 2 mm) is supposed to be maintained, settling at an approximately steady position within the vessel (dynamic equilibrium of the operative forces gravity, buoyancy and drag, while maintaining a state of continuous freefall; see Experiments and Terminal Velocity subsection). According to experimental observations (Freed et al., 1997; Obradovic et al., 2000), the fluid filling the rotating vessel laps against the tissue, which has a position held constant in time with the flat, circular area perpendicular to the direction of motion. The specimen is supposed to maintain axisymmetric shape during the growth process, its symmetry axis being coincident with the symmetry axis of the cylindrical scaffold initially used to seed the chondrocytes. The velocity field is supposed to be uniform and parallel to the aforementioned axis at a sufficient distance (about 1 cm) from the construct (undisturbed conditions). Its intensity therein is assumed to be equal to the terminal velocity computed as discussed in the Experiments and Terminal Velocity subsection.

A 20-mm-high by 20-mm-wide (radius = 10 mm) computational domain has been simulated. Figure 2 shows the geometry of the computational domain and the boundary conditions (note that, due to the axisymmetry of the model, for the sake of simplicity and brevity, only half of the generic meridian plane is shown in Fig. 2): $y = 0$ corresponds to the symmetry axis, $y = 1$ to the distance from the axis at which undisturbed flow conditions prevail, $x = 0$ corresponds to the ''inflow'' section (in the laboratory the construct holds a fixed position and the fluid moves upward in the direction

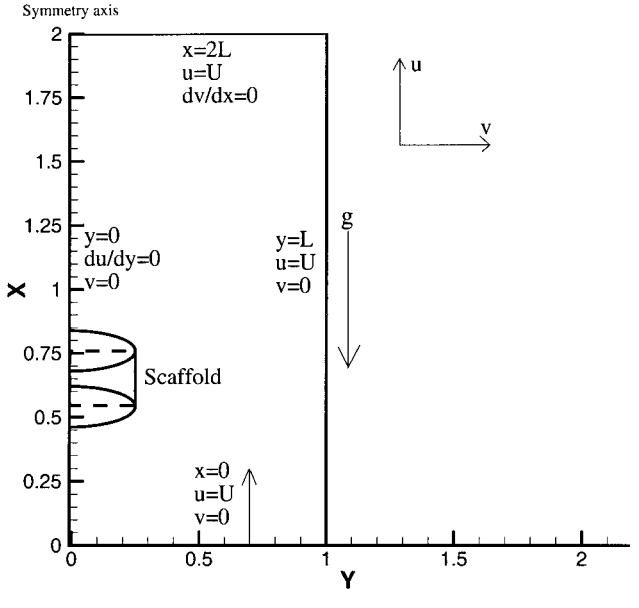

Figure 2. Computational domain and boundary conditions (U is the terminal velocity and u and v are the velocity components in axial and radial direction respectively).

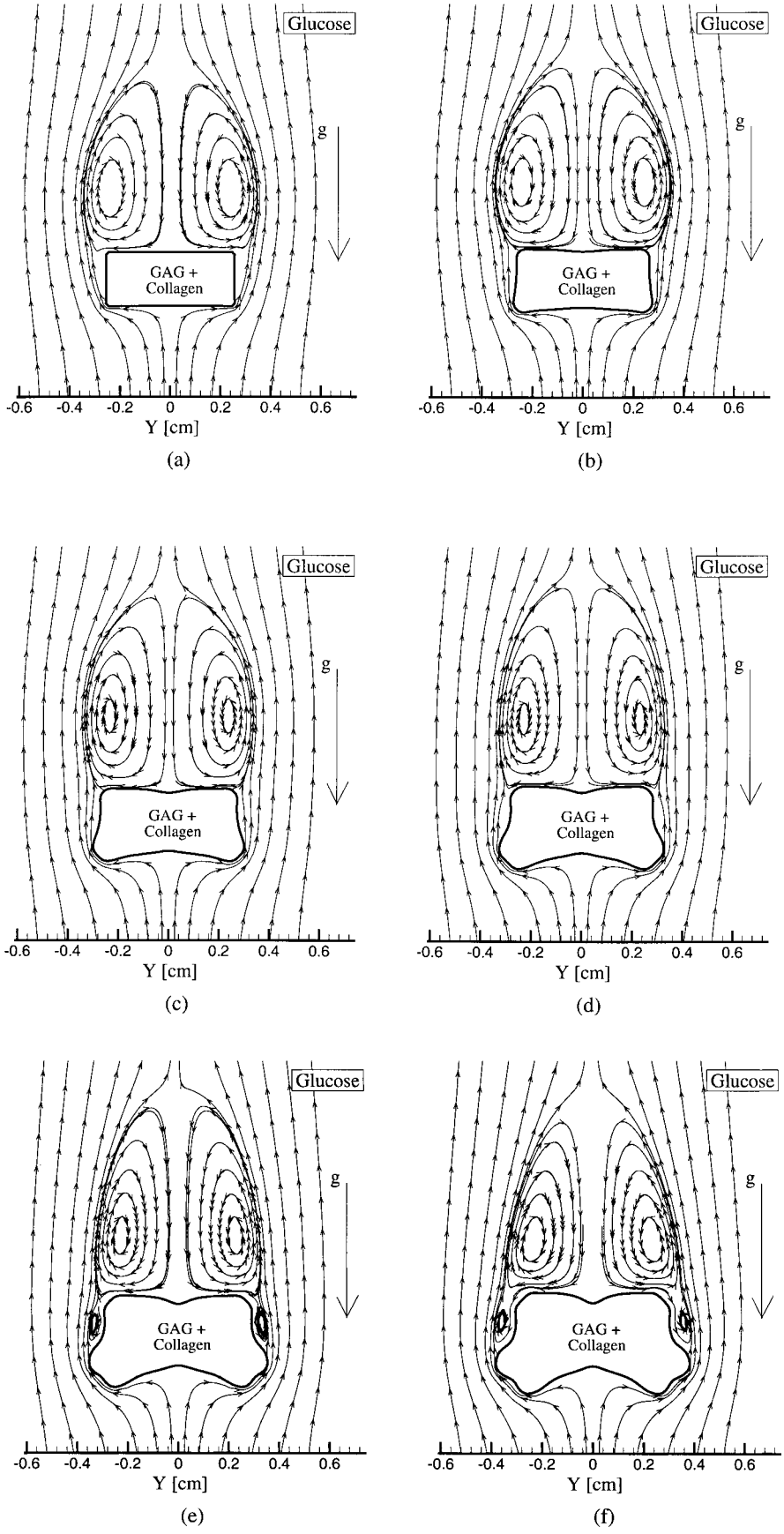

Figure 3. Snapshots of growing tissue and surrounding velocity field: (a) t = 10 days; (b) t = 16 [days], (c) t = 22 days; (d) t = 28 days; (e) t = 34 days; (f) t = 40 days. With regard the experiments by Obradovic et al. (2000), note that (a) and (f) corresponding to their initial condition (scaffold) and to construct cultured for 6 weeks, respectively.

opposite to the gravity force), and correspondingly $x = 2$ is the ''outflow'' section.

For $y = 0$, ''mirror'' boundary conditions are imposed; that is, the radial velocity component (v) is zero and the axial one (u) does not change across the axis ($du/dy = 0$); for $y = 1$, undisturbed flow conditions are imposed, that is, $v = 0$ (the undisturbed flow does not have a radial velocity component) and $u = U$; for $x = 0$, undisturbed flow conditions are again imposed; for $x = 2$ (outflow section), the axial velocity component is equal to the terminal velocity as for the inflow section (the volumetric rate of flow has to be constant throughout the system because the liquid is an incompressible fluid), but a nonzero radial velocity component may be present due to the interaction of the moving fluid with the obstruction created by the presence of the organic construct. For this reason, the condition $dv/dx = 0$ is imposed therein (this condition guarantees that the radial velocity at the outflow section is free to change according to the behavior of the wake produced beyond the specimen).

On the basis of a grid-refinement study (not shown for the sake of brevity) a mesh with 200 points in the axial direction and 100 points in radial direction is used. Growth is obtained from a solution with initial concentration $C_{\text{glucose}(o)} = 4.5 \cdot 10^{-3}$ g cm^{-3} (the diffusion coefficient is $D_{\text{glucose}} = 6.7 \cdot 10^{-6}$ cm^2 s^{-1}, the kinematic viscosity is $\nu = 8 \cdot 10^{-3}$ cm^2 s^{-1}). The frontier of the domain is supposed to be at constant concentration during the growth process (i.e., $C_{\text{glucose}} = C_{\text{glucose}(o)}$).

In the experiments (see Obradovic et al., 2000) cells proliferated over the first 5 to 7 days. Only after cell growth ceased did the cells begin to separate themselves by synthesizing matrix components (GAG + collagen). Therefore, the investigators focused on the period between the first 10 days of growth and 6 weeks (42 days). The same period (even if computationally very expensive) is simulated in the present study.

Note that, clearly (the present mathematical model and associated numerical method are original and are applied herein for the first time) no data are available from the literature regarding the value to assign to the kinetic coefficient in Eq. (12).

This value has been determined in a unique manner: Several simulations have been carried out for different values of this parameter, then the effective λ has been selected out on the basis of the experimentally determined rate of growth of the specimen size (the size of the construct increased at a constant rate of 70 μm/day = $8.1 \cdot 10^{-8}$ cm s^{-1} = 8.1 Å s^{-1}; see Obradovic et al., 2000). This method has led to $\lambda = 3 \cdot 10^{-6}$ cm s^{-1} and $\tilde{a} = 3 \cdot 10^{-9}$. Validation of the aforementioned procedure has been provided by the very good agreement of numerical predictions obtained using these values with the experimentally found morphological data. The two parameters, λ and $\tilde{a}$ have been determined from the data of Obradovic et al. (2000) pertaining to the rate of increase of tissue size. It is worthwhile to point out how this rate is an average shape-independent parameter. In contrast, the criterion to conclude that the model is correct has been based on the morphological (shape-change) evolution of the tissue. The numerical results are able to reproduce the morphological evolution observed by Obradovic et al. (2000), even if they provided no data with regard to laws and kinetics modeling the shape evolution.

The growth process is shown in Fig. 3. Each figure part (a–e) corresponds to a different snapshot of the growth process.

A toroidal vortex roll is created behind the growing specimen. This behavior is due to the obstruction created in the fluid flow by the presence of the disk-shaped tissue with its circular area perpendicular to the direction of motion. The toroidal convection roll appears in the generic meridian plane in the form of two vortices located behind the body in the downstream direction. The two vortices are embedded in a low-velocity region hereafter referred to as the ''wake.''

Note that the interaction of the flow entering into the computational domain from the lower boundary with the axisymmetric body embedded in the inner space of the reactor leads to two main effects. One is the aforementioned creation of a wake, the second is an effect of deceleration/acceleration of the fluid. The flow is strongly curved because it enters the computational domain directed along x and is then forced to skirt around the construct. Due to this path and its initial conditions, the fluid is initially decelerated along x up to the stagnation conditions on the tissue surface; it is then accelerated in the downstream direction due to the cross-sectional area reduction associated with the presence of the specimen. This structure is crucial in determining the distribution of surface shear stress and thus the growth behavior.

The simulations show that corners and edges of the tissue are more readily supplied with solute (glucose) than the center of the sides (this leads to morphological instability and to a macroscopic depression around the center of the faces; see Fig. 3). This is due to the pattern of the nutrient concentration field around the growing construct. As previously discussed, absorption of the solute into the tissue causes a local depletion in concentration and a solutal

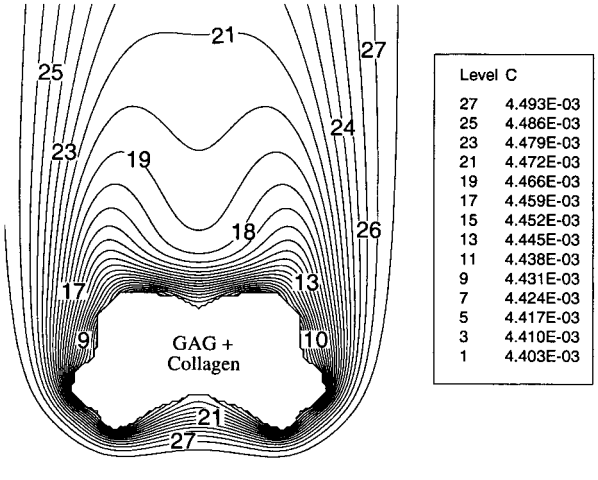

Figure 4. Glucose concentration distribution (t = 40 days).

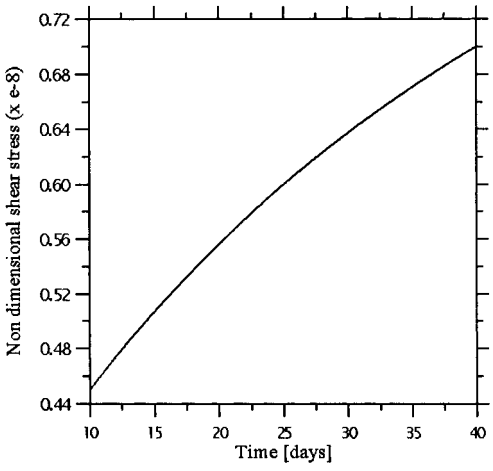

Figure 5. Maximum shear stress versus t.

concentration gradient to form between the bulk solution and the growth interface. The ''steepness'' of the gradient determines the rate of solute transport to the growth interface, the steepness being maximal around the corners (see Fig. 4). Superimposed on this is the fact that a protuberance on the interface encounters a higher shear stress and, according to Eqs. (12) and (16), grows faster than a depression, which encounters a lower shear stress.

This behavior is evident in Figure 6a, which shows the growth habit simulation and progression of cartilaginous matrix deposition. Note that the onset of morphological instabilities and the existence of ''depressions'' around the center of the faces of growing tissues (shown by the present numerical results) is in very good agreement with the experimental results of Freed et al. (1997) and Obradovic et al. (2000) (see Fig. 6b). Figure 6, in particular, allows for a comparison of the numerical and experimental results (Obradovic et al., 2000) by highlighting some characteristic points along the border of the construct (consider the correspondence between the points A–F in Fig. 6a and b).

It is worthwhile to point out that the ''depth'' of the face depressions is proportional to the size of the specimen; that is, it increases during growth (Fig. 6a).

As time passes and the tissue widens, disturbance in the flow field produced by the presence of the construct becomes larger. This behavior in turn increases the value of the shear stresses responsible for the growth of protuberances on the surface (see Fig. 5).

A detailed description of these phenomena requires a separation of the analysis for the different faces of the construct.

The ''face'' (average) growth rate exhibits a different value according to orientation of the face with respect to the main direction of the flow; an important parameter is the relative direction of the different faces, which induces varying conditions for each face.

Figure 7 shows in detail how the convection effect results in higher local shear stresses near the surface where the flow is incoming (lower face) and in lower shear stresses near the surface where the flow is outgoing (upper face). This behavior can be explained based on the fact that the upper side faces a region where recirculating flow occurs, and therefore the fluid is in close-to-stagnation conditions. For this reason the shear stresses causing growth there are weakened and, correspondingly, the growth rate is reduced. For the same reasons, the onset of morphological instabilities is prevented for the upper side (the tissue surface facing the wake is almost planar and without irregularities).

Moreover, it is noteworthy that, as time passes, the toroidal vortex close to the upper side becomes larger. The expansion of the wake is strictly related to the behavior of the tissue that puffs out due to growth.

At the same time, and for the same reason (increasing size of the sample), the shear stresses (and associated growth rates) at the corners of the lower surface increase. This is due to the acceleration of the flow around the corners induced by the progressive reduction of the available cross-sectional area in a direction perpendicular to the flow and provides a

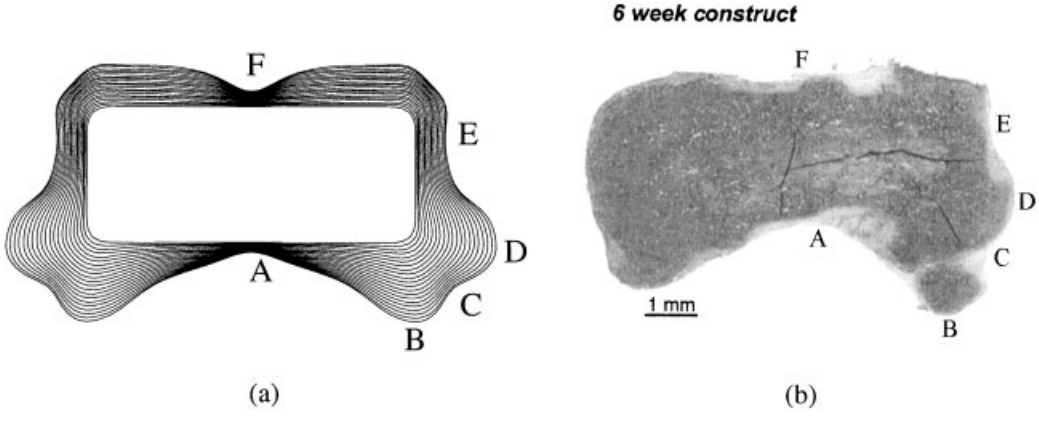

Figure 6. (a) Tissue growth habit simulation and progression of cartilaginous matrix deposition: snapshots of the tissue shape versus time ($\Delta t = 5.2 \cdot 10^4$ seconds, (b) experimental histological cross-section of cartilage construct cultured for 6 weeks (Obradovic et al., 2000). (Reproduced with permission of the American Institute of Chemical Engineers. Copyright © 2000 AIChE. All rights reserved.)

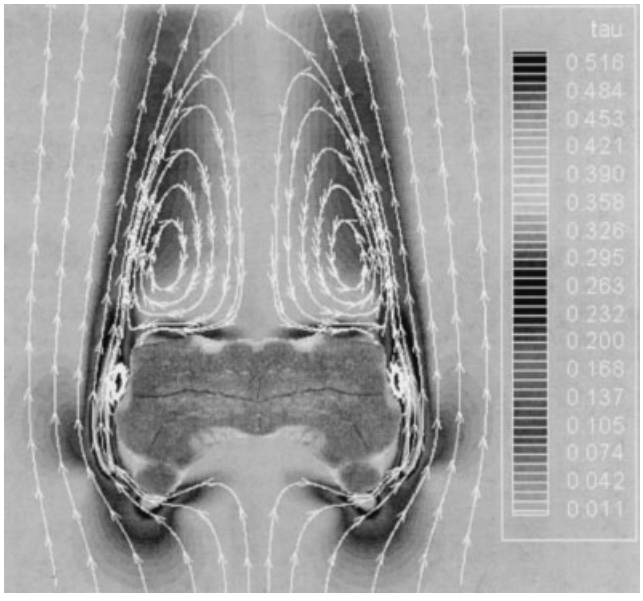

Figure 7. Velocity field and nondimensional shear-stress distribution ($\times 10^{-8}$; $t = 40$ days). Experimental histological cross-section of cartilage construct cultured for 6 weeks, obtained by Obradovic et al. (2000), is superimposed on the independently computed tissue shape and on the velocity and shear-stress distributions at the same time.

theoretical explanation for the trend shown in Figure 5. It is noteworthy how expansion of the lower edges in the radial direction (see Fig. 3e–f) is also responsible for the presence of an additional secondary small vortex ring circumferentially wrapped around the construct.

In Figure 7, the experimental histological cross-section of cartilage construct cultured for 6 weeks (Obradovic et al., 2000) is superimposed on the independently computed tissue shape and on the velocity and shear-stress distributions at the same time. This artifice is used to highlight how the numerical and experimental results are in very good agreement and how edges and protuberances correspond to the regions of high shear stress. The superposition provides an excellent validation of the present shear-stress-based kinetic model and associated moving boundary (CFD) computational method. Note that the left side of the experimental image has been replaced by the mirror image of the right side. This artifice has been used because the numerical computations are axisymmetric. For this reason they cannot reproduce the weak asymmetry that may characterize the specimen from an experimental point of view. The prediction of weak asymmetries arising in the final shape of the tissue due to environmental factors, such as 3D instabilities of the flow field in the wake behind the specimen, Coriolis forces, terminal velocity nonparallel to the symmetry axis, small asymmetries in initial shape of the scaffold, curvature of flow due to rotation of the vessel, etc., is not possible on the basis of the present model. Three-dimensional computations would be necessary. In that case, however, massively parallel supercalculus would be necessary instead of normal parallel supecalculus. This area of study is the subject of forthcoming analyses.

DISCUSSION

In the translation of mechanical culture conditions into tissue effects, several lines of evidence seem to support a role for shear stress. The present analysis gives a definitive answer to this question providing heretofore unseen theoretical background supported by numerical simulations. In light of the arguments pointed out in the Numerical Simulations subsection, the fluid shear distribution turns out to be crucial for the surface absorption kinetics and for the overall tissue-growth process. It acts by modifying the ''internal cell division'' and ''addition of extracellular matrix'' mechanisms responsible for tissue enlargement and leads to different growth rates for the different sides of the specimen and to the onset of morphological instability (i.e., depressions and/or protuberances of the tissue/culture-medium interface). Moreover, according to the present analysis, the shear-stress distribution is not constant in time but changes due to the increased size of the organic construct. The interplay between the increasing size of the tissue and the structure of the convective field is essential in determining the time evolution of its shape.

It has been shown that the size of the growing specimen plays a ''critical role'' in determining the intensity of convection and of the shear stresses. Convective effects, in turn, are found to impact growth rates, particle size, and morphology, as well as the mechanisms driving growth.

The present analysis completely supports, by quantitative modeling and computations, Freed's supposition (Freed et al., 1997) about the effect of fluid shear stress in her experiments: On Mir, the constructs were exposed to uniform shear and mass transfer at all surfaces such that the tissue grew equally in all directions, whereas, on Earth, the particular fluid-dynamic environment increases shear and mass transfer circumferentially such that the tissue tends to grow preferentially in the radial direction (around the lower corners).

For the first time, the experiments of Freed et al. (1997) proved the effect of the fluid-dynamic environment on growth and morphological evolution of tissue through direct comparison of experiments carried out in the true weightlessness of space and on the ground. On the basis of the lines of evidence supported by cross-check of these experiments and by the present computations, some highly relevant conclusions can be drawn. On the ground, the rotating vessel does not actually cancel the effects of gravity, because the endless freefall of the specimen through the liquid leads to a convective pattern that, due to shear-stress-dependent surface kinetics, influences the final shape of the biological construct.

CONCLUSIONS

A mathematical model has been carefully developed for the case of growth of organic tissues that are extremely complex physical–chemical systems and whose properties may vary as a function of many environmental influences. The case of

the rotating bioreactor has been investigated because the rotating-wall vessel largely solves the primary challenge of suspension culture: to suspend cells and microcarriers while providing adequate nutrition and oxygenation.

An original volume-of-fraction method specifically designed for the case under investigation has been introduced and applied to recent important experiments corresponding to the growth of a cartilage construct. This method, which eliminates the need for separate equations in each phase by establishing conservation equations that are universally valid, allows a fixed-grid solution to be undertaken and is therefore able to utilize standard solution procedures for the fluid flow and species equations directly, without resorting to mathematical manipulations and transformations (this feature, on the other hand, facilitates a parallel implementation of the code based on a grid-partition strategy).

In the OTGVOF method, the ''phase-field'' variable, ϕ, is computed using incorporation kinetics at the surface of the biological tissue. These conditions are coupled to the exchange mass flux at the interface and lead to the introduction of a group of differential equations for the nutrient concentration around the specimen and the evolution of matrix mass displacement.

The model has been based on reasonable assumptions and on parameters that were experimentally determined. In particular, the ''sensitivity'' of the surface (i.e., growth rate) of the organic tissue to shear stress has been taken into account. The ''physical forces'' due to fluid motion induce changes in cell metabolism and function. The stress environment elicits a physiological response from the cells that are the building blocks of the construct, causing them to produce extracellular matrix (ECM). Accordingly, for the numerical simulations, the growth velocity and/or the ''growth law'' were not been directly imposed but resulted from conditions related to solute transport and shear-stress distribution (i.e., mass and momentum transfer).

It is generally accepted that the growth of organic tissue depends in part on biochemical factors. However, the precise relationships that govern growth in general are not known. The results presented herein fit with the processes that control tissue development. The consistency of model predictions with experimental data suggests that rate-controlling steps have been taken into account, and that simplifications do not distort actual behavior. The method has proven to be able to predict morphology instabilities (i.e., habit/shape change) of the tissue. An analysis of the distribution of the local growth rate along the sides of the specimen has been carried out. The growth rate was found to be nonuniform across the faces (growth rate is always lower at the center than at the corner). This follows because the ''steepness'' of the concentration gradient and the local fluid-dynamic shear stress determine the rate of incorporation and conversion of the nutrients into the tissue main components (the steepness of the feeding concentration gradient and the fluid stress being maximum around the corners).

The role of the changes in size of the sample in determining the intensity of the convective field and its structure (the increasing size of the constructs tends to strengthen the shear stresses at the lower corners and to weaken them on the upper surface) has been pointed out.

Determining the growth laws and models is central to understanding how environmental conditions affect growth. Moreover, this knowledge is essential for growing replacement organic constructs in vitro through the techniques of tissue engineering. The present investigation demonstrates both the potential and challenges of mathematical modeling of in vitro organic tissue growth.

The proposed models and methods exhibit heretofore unseen capabilities to predict and elucidate experimental observations and to identify cause-and-effect relationships; that is, they give insight into the mechanisms driving the phenomena under investigation. Of course, further investigation is needed to couple the present techniques with other, existing ones by taking into account the effect of internal fiber stress of the tissue and the complex 3D fluid-dynamics occurring in the rotating vessel system.

The author thanks the reviewers for their very constructive comments and Dr. Gordana Vunjak-Novakovic for making available some important experimental data.

References

Beckermann C, Diepers H-J, Steinbach I, Karma A, Tong X. 1999. Modeling melt convection in phase-field simulations of solidification. J Comput Phys 154:468–496.

Begley CM, Kleis SJ. 2000. The fluid dynamic and shear environment in the NASA/JSC rotating-wall perfused vessel bioreactor. Biotechnol Bioeng 70:32–40.

Bennon WD, Incropera FP. 1987. A continuum model for momentum, heat and species transport in binary solid–liquid phase change systems—I. Model formulation. Int J Heat Mass Transfer 30:2161–2170.

Briegleb W. 1988. Ground-born methods in gravitational cell biology. The Physiologist 31:44–47.

Briegleb W. 1992. Some qualitative and quantitative aspects of the fast-rotating clinostat as a research tool. ASGSB Bull 52:23–30.

Clift R, Grace JR, Weber ME. 1978. Bubbles, drops and particles. New York: Academic Press.

Cogoli M. 1992. The fast rotating clinostat: A history of its use in gravitational biology and a comparison of ground-based and flight experiment results. ASGSB Bull 52:59–67.

Coimbra CFM, Kobayashi MH. 2002. On the viscous motion of a small particle in a rotating cylinder. J Fluid Mech 469:257–286.

Freed LE, Langer R, Martin I, Pellis NR, Vunjak-Novakovic G. 1997. Tissue engineering of cartilage in space. Proc Natl Acad Sci USA 94: 13885–13890.

Fung YC. 1990. Biomechanics: Motion, flow, stress, growth. New York: Springer.

Gao H, Ayyaswamy PS, Ducheyne P. 1997a. Dynamics of a microcarrier particle in the simulated microgravity environment of a rotating wall vessel. Microgravity Sci Technol X:154–165.

Gao H, Ayyaswamy PS, Ducheyne P. 1997b. Numerical simulation of global diffusive mass transfer in a rotating wall vessel bioreactor. Adv Heat Mass Transfer Biotechnol 37:59–67.

Gueyffier D, Li J, Nadim A, Scardovelli S, Zaleski S. 1999. Volume of fluid interface tracking with smoothed surface stress methods for three-dimensional flows. J Comput Phys 152:423–456.

Hammond TG, Hammond JM. 2001. Optimized suspension culture: The rotating-wall vessel. Am J Physiol Renal Physiol 281:F12–F25.

Harlow FH, Welch JE. 1965. Numerical calculation of time-dependent

viscous incompressible flow with free surface. Phys Fluids 8: 2182–2189.
Helmrich A, Barnes D. 1998. Animal cell culture equipment and techniques. Meth Cell Biol 57:3–17.
Hemmersbach-Krause R, Briegleb W, Häder D-P, Vogel K, Grothe D, Meyer I. 1993. Orientation of paramecium under the conditions of weightlessness. J Euk Microbiol 40:439–446.
Kim YT, Goldenfeld N, Dantzig J. 2000. Computation of dendritic microstructures using a level set method. Phys Rev E 62:2471–2474.
Kleis SJ, Schreck S, Nerem RM. 1990. A viscous pump bioreactor. Biotechnol Bioeng 36:771–777.
Kordyum EL. 1994. Effects of altered gravity on plant cell processes: Results of recent space and clinostatic experiments. Adv Space Res 14:77–85.
Kothe DB, Ferrell RC, Turner JA, Mosso SJ. 1997. A high resolution finite volume method for efficient parallel simulation of casting processes on unstructured meshes. Presented at the eighth SIAM conference on Parallel Processing for Scientific Computing, Minneapolis, MN, 1997.
Kunitake R, Suzuki A, Ichihashi H, Matsuda S, Hirai O, Morimoto K. 1997. Fully-automated roller bottle handling system for large scale culture of mammalian cells. J Biotechnol 52:289–294.
Lappa M. 1997. Strategies for parallelizing the three-dimensional Navier–Stokes equations on the Cray T3E. Sci Supercomput CINECA 11: 326–340.
Lappa M. 2003. Growth and mutual interference of protein seeds under reduced gravity conditions. Phys Fluids 15:1046–1057.
Lappa M, Savino R. 1999. Parallel solution of three-dimensional Marangoni flow in liquid bridges. Int J Numer Meth Fluids 31:911–925.
Lappa M, Savino R. 2002. 3D analysis of crystal/melt interface shape and Marangoni flow instability in solidifying liquid bridges. J Comput Phys 181:1–24.
Mather JP. 1998. Laboratory scaleup of cell cultures 0.5–50 liters. Meth Cell Biol 57:219–227.
Meaney DF, Johnston ED, Litt M, Pollack SR. 1998. Experimental and numerical investigations of microcarrier motions in simulated microgravity. Adv Heat Mass Transfer Biotechnol 63:21–27.
Obradovic B, Meldon JH, Freed LE, Vunjak-Novakovic G. 2000. Glycosaminoglycan deposition in engineered cartilage: Experiments and mathematical model. AIChE J 46:1860–1871.
Osher S, Fedkiw R. 2002. The level set method and dynamic implicit surfaces. New York: Springer.
Pollack SR, Meaney DF, Levine EM, Litt M, Johnston ED. 2000. Numerical model and experimental validation of microcarrier motion in a rotating bioreactor. Tissue Eng 6:519–530.
Pusey ML, Snyder RS, Naumann R. 1986. Protein crystal growth: Growth kinetics for tetragonal lysozyme crystals. J Biol Chem 261:6524–6529.
Rider WJ, Kothe DB. 1998. Reconstructing volume tracking. J Comput Phys 141:112–152.
Rodriguez EK, Hoger A, McCulloch A. 1994. Stress-dependent finite growth in soft elastic tissues. J Biomech 27:455–467.
Rosenberger F. 1986. Inorganic and protein crystal growth: Similarities and differences. J Cryst Growth 76:618–636.
Sethian J. 1999. Level set methods and fast marching methods. New York: Cambridge University Press.
Taber LA. 1998a. Biomechanical growth laws for muscle tissue. J Theor Biol 193:201–213.
Taber LA. 1998b. A model for aortic growth based on fluid shear and fiber stresses. J Biochem Eng 120:348–354.
Taber LA, Chabert S. Theoretical and experimental study of growth and remodeling in the developing heart. Biomech Model Mechanobiol (in press).
Todd P, Gruener R. 1992. Clinostats and centrifuges. ASGSB Bull 52: 84–93.
Topper JN, Gimbrone MA Jr. 1999. Blood flow and vascular gene expression: Fluid shear stress as a modulator of endothelial phenotype. Mol Med Today 5:40–46.
Udaykumar HS, Mittal R, Shyy W. 1999. Computation of solid–liquid phase fronts in the sharp interface limit on fixed grids. J Comput Phys 153:535–574.
Wolf DA, Schwartz RP. 1991. Analysis of gravity-induced particle motion and fluid perfusion flow in the NASA-designed rotating zero-headspace tissue culture vessel. NASA Technical Paper 3143.
Wolf DA, Schwartz RP. 1992. Experimental measurement of the orbital paths of particles sedimenting within a rotating viscous fluid as influenced by gravity. NASA Technical Paper 3200.